

# Measurement of the forbidden tensor polarizability of Cs using an all-optical Ramsey resonance technique

C. Ospelkaus,\* U. Rasbach,<sup>†</sup> and A. Weis<sup>‡</sup>

*Département de Physique, Université de Fribourg, 1700 Fribourg / Switzerland*

Spin polarization created by optical pumping in a thermal cesium beam is allowed to evolve in static magnetic and / or electric fields and is probed downstream by a circularly polarized probe beam. As a function of the magnetic field strength, a typical Ramsey fringe pattern is observed. Phase shifts due to the interaction of a static electric field are detected as fringe shifts, which yields a new method for the measurement of the tensor polarizability  $\alpha_2$  of the ground state of alkali atoms. We show that the electric tensor polarizability of  $^{133}\text{Cs}$  can be measured with a statistical uncertainty of 0.7%. Absolute measurements are currently limited by systematic effects.

PACS numbers: 32.60.+i, 12.20.Fv

## INTRODUCTION

Alkali atoms - due to their single weakly bound valence electron - have the largest electric polarizabilities of all elements. These polarizabilities arise as a result of second order perturbation theory of the Stark interaction and manifest themselves as  $\mathcal{E}^2$ -dependent shifts of the energy levels induced by an external electric field  $\mathcal{E}$ . Because of the spherical symmetry of the alkali  $^2\text{S}_{1/2}$  ground state configuration, the Stark effect for these elements has a scalar nature, which is conventionally parametrized in terms of a scalar polarizability  $\alpha_0$ . All hyperfine sublevels of the ground state experience the same shift and their degeneracy is not lifted by the electric field.

In third order perturbation theory, however, the hyperfine (Fermi contact, dipole-dipole and electric quadrupole) interaction, together with the Stark interaction, leads to a strongly suppressed (six to seven orders of magnitude with respect to the scalar polarizability), but finite value of the tensor polarizability  $\alpha_2$ . The electric field induced shift of the hyperfine Zeeman component  $|F, M_F\rangle$  is given by

$$\Delta E(F, M_F) = -\frac{1}{2}\alpha(F, M_F)\mathcal{E}^2, \quad (1)$$

where the polarizability  $\alpha$  has scalar and tensor parts

$$\alpha(F, M_F) = \alpha_0(F) + \alpha_2(F) \frac{3M_F^2 - F(F+1)}{F(2F-1)}. \quad (2)$$

The scalar polarizability  $\alpha_0(F)$  contains an  $F$ -dependent third order correction (from the Fermi contact interaction) to the second order scalar polarizability. This correction leads to a differential shift of the two hyperfine levels  $F_{\pm} = I \pm J$ , and has been measured on the Cs clock transitions [1, 2]. This effect is approximately 2 orders of magnitude larger than the tensor effect discussed here. For Cs atoms in typical laboratory fields in the range of a few 10 kV/cm, one expects sublevel splittings due to the tensor polarizability on the order of 1 Hz. The tensor polarizabilities of several alkali elements were measured

in the 1960's using atomic beams and conventional Ramsey resonance spectroscopy. However, the authors of [3] found large discrepancies between the predicted [4, 5] theoretical values of  $\alpha_2$  and their experimental results.

The novel Ramsey resonance technique presented here is an all-optical technique, which does not use radio-frequency (r.f.) or microwave fields and allows to study the tensor Stark effect of the two ground state hyperfine levels individually. Compared to the conventional Ramsey technique our method avoids r.f. power dependent systematic effects that are due, e.g., to multi-(r.f.) photon processes (cf. [3]).

## FARADAY-RAMSEY SPECTROSCOPY

The measurements presented in this paper were performed using an optical pump-probe technique in a thermal cesium beam (figure 1). A circularly polarized pump beam resonant with a hyperfine component of the Cs D<sub>2</sub> line (852 nm) produces spin polarization  $\vec{S} = \langle \vec{F} \rangle$  oriented along the  $\vec{k}$ -vector of the pump beam and perpendicular to the atomic velocity  $\vec{v}$ . When exposed to a static magnetic field  $\vec{B}$ , the spin polarization precesses around the magnetic field at the Larmor frequency  $\omega_B = \gamma_F \cdot |\vec{B}|$ .

The spin polarization is measured downstream by recording the transmission of a weak circularly polarized probe laser beam. The absorption depends on the projection of the velocity averaged spin polarization on the probe laser beam. The magnetic field dependence of the transmitted intensity then leads to a damped oscillatory pattern (Ramsey fringes) symmetric around  $B = 0$ . For practical purposes it is more convenient to work with a dispersive (antisymmetric around  $B = 0$ ) fringe pattern. Such a line shape can be generated by applying a small amplitude modulation to the magnetic field and detecting the transmitted intensity using a lock-in amplifier locked to the modulation frequency. For  $\vartheta = 90^\circ$  the resulting

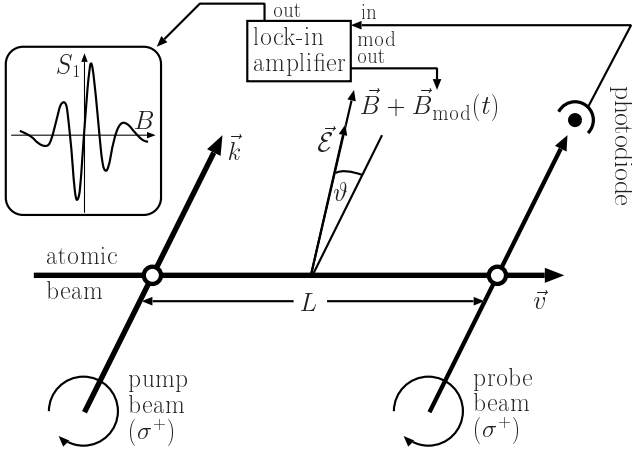


FIG. 1: Experimental setup of the pump-probe experiment with circularly polarized light. The insert shows a typical experimental recording of the probe beam absorption as a function of the magnetic field. With  $L = 30\text{ cm}$ , the period of the oscillatory structure is approximately 200 nT.

lineshape  $S_1(B)$  is given by

$$S_1(B) \propto \int_0^\infty \sin(\gamma_F B \frac{L}{v}) \frac{\rho(v)}{v} dv,$$

where  $\rho(v) dv$  is the velocity distribution of the atomic density in the probe region. A typical experimental recording of such a Ramsey fringe pattern is shown as insert in figure 1. The steep central zero-crossing of this pattern is a very sensitive discriminant for the measurement of other (e.g.  $\vec{\mathcal{E}}$ -field induced) interactions which produce differential phase shifts of the magnetic sub-levels of the ground state. Previous experiments using this technique were carried out with linearly polarized laser beams and detected the rotation of the probe beam polarization. The description of the nonlinear Faraday-effect as a three step process [6, 7] together with Ramsey's idea of separated fields gave this method the name of Faraday-Ramsey spectroscopy (FRS) [8, 9]. FRS has been used to measure the Aharonov-Casher phase shift of  $^{85}\text{Rb}$  [10].

The key idea of the experimental technique used to measure the tensor polarizability is the following: In the interaction zone the Cs beam is exposed to parallel static electric  $\vec{\mathcal{E}}$  and magnetic  $\vec{B}$  fields oriented at an angle  $\vartheta$  with respect to the  $\vec{k}$ -vector of the pump beam. When  $\vec{\mathcal{E}} = 0$  a feed-back loop actively stabilizes the magnetic field to the center of the dispersive central Ramsey fringe. Any additional phase shift induced by the electric field is then compensated by an automatic adjustment of the magnetic field. The corresponding compensation current  $I_{\text{FB}}$  in the field generating coils is the signal of interest.

For the quantitative interpretation of this compensation technique one has to know the electric field equiv-

alent of the magnetic compensation field. A straightforward calculation shows that the field-induced change of the probe absorption coefficient for a monochromatic beam prepared in the pump region in the stretched hyperfine state  $|F, M_F = F\rangle$  can be expressed as

$$S_1(\Phi_B, \Phi_E) \propto \Phi_B \sin^2 \vartheta + (2F - 1)\Phi_E \cos \vartheta \sin^2 \vartheta, \quad (3)$$

where the magnetic and electric phases  $\Phi_{B,E}$  are given by

$$\Phi_B = \gamma_F \frac{\int B dl}{v} \quad \text{and} \quad \Phi_E = -\frac{3}{2F(2F - 1)} \frac{\alpha_2}{\hbar} \frac{\int \mathcal{E}^2 dl}{v}.$$

The integrals are over the atomic trajectories between the pump and probe regions. As both phases have the same dependence on the atomic velocity  $v$  any velocity averaging will produce a mere proportionality factor, which is irrelevant for the following discussion, and will thus be omitted. Equation 3 - derived under the assumption  $\Phi_{B,E} \ll 1$  - allows to define the optimal geometry and to calibrate the electric shift in terms of the magnetic compensation. As the feedback loop in the experiment adjusts the magnetic field such that  $S_1(\Phi_B, \Phi_E) = 0$ , the signal  $S$  is most sensitive to  $\Phi_E$ , i.e., to the tensor polarizability when  $\vartheta$  is chosen to be the magic angle  $\vartheta_m$ , which satisfies  $3 \cos^2 \vartheta_m - 1 = 0$  and which maximizes the electric contribution in Equation 3. The same equation can also be used to define the magnetic equivalent of the electric phase shift, which implies

$$\frac{\alpha_2}{\hbar} = \frac{F \cdot \gamma_F}{3\pi \cos \vartheta} \cdot \frac{\int B dl}{\int \mathcal{E}^2 dl} \quad (4)$$

$$\equiv \frac{F \cdot \gamma_F}{3\pi \cos \vartheta} \cdot \frac{\beta}{\varepsilon} \cdot \frac{I_{\text{FB}}}{U_{\text{HV}}^2}. \quad (5)$$

Equation 5 can be understood as follows: the first factor depends on specific atomic properties and on the geometry of the experimental arrangement, while the second and third factors contain calibration constants  $\beta$  and  $\varepsilon$ , which relate the field integrals  $\int B dl$  and  $\int \mathcal{E}^2 dl$  to the feedback current  $I_{\text{FB}}$  and to the square of the applied high voltage  $U_{\text{HV}}$  respectively. Once the calibration constants are known, the tensor polarizability can be inferred from the measured dependence of  $I_{\text{FB}}$  on  $U_{\text{HV}}$ .

## EXPERIMENTAL SETUP

In the experiment, the pump and probe beams are delivered by the same extended cavity diode laser locked to the  $F = 4 \rightarrow F' = 5$  hyperfine component of the Cs D<sub>2</sub> transition using standard saturated absorption spectroscopy in an auxiliary vapor cell. The laser beam is transferred to the experiment proper by an optical fiber which also serves as a mode cleaner. The output intensity of the fiber is actively stabilized by a feed-back

circuit controlling the input intensity with an acousto-optic modulator. The atomic beam is produced by a reflux oven [11] operated at a temperature of 130°C and delivering a beam with a divergence of 40 mrad. Between the pump and probe zones – separated by a 30 cm long interaction zone – the atomic beam propagates in a 7 cm diameter electrically grounded tube, which contains a pair of polished copper electrodes that can be rotated around the atomic beam axis. One of the electrodes is grounded, while the other electrode is connected to a computer-controlled high voltage power supply that allows to apply electric fields up to 20 kV/cm. Two grounded diaphragms are located between the electrodes and the laser beams to ensure that the pump and probe interactions take place in an electric field-free environment. A solenoid wound on the beam tube and two pairs of rectangular coils allow to apply magnetic fields of arbitrary orientation and/or to shield unwanted field components. All coils extend over the pump and probe regions. The whole set-up is enclosed in a double cylindrical mu-metal shield. The data acquisition (high voltage and feedback current) is controlled by a PC and the robustness of the laser frequency lock allows the experiment to be run overnight without user intervention.

## SYSTEMATIC STUDIES AND RESULTS

When  $\vartheta \neq 90^\circ$  the motional magnetic field seen by the atoms moving through the static electric field leads to an additional magnetic phase shift, which is proportional to the electric field, i.e. to  $U_{\text{HV}}$ . This linear Stark effect is also known as Aharonov-Casher phase shift [10]. A further noisy background may come from slowly drifting magnetic offset fields. The measurements were therefore performed in a way that allows to eliminate these backgrounds from the recorded data.

In a typical experimental run (12 hours) the data acquisition software controls the high voltage power supply by applying 5 discrete voltages  $U_i$  ( $i = 1, \dots, 5$ ) to the electrodes, each with both polarities. Part of an experimental run, which consists of individual two minute long recordings is shown in figure 2. We start with  $U_{\text{HV}} = 0$  and record  $I_{\text{FB}}$ . Then the software applies the voltage  $U_{\text{HV}} = U_{i=1}$  and records  $I_{\text{FB}}$  for another two minutes, after which the polarity is reversed and  $I_{\text{FB}}$  is recorded with  $U_{\text{HV}} = -U_{i=1}$ . In the next step  $i$  is incremented by 1 and the cycle starts again with  $U_{\text{HV}} = 0$ . When  $i = 5$  is reached (end of figure 2), the whole procedure is repeated. The integration time of 2 minutes was chosen after a detailed study of the system stability in terms of the Allan variance of  $I_{\text{FB}}$ , which showed a minimal value for integration times between 100 and 200 seconds.

Figure 2 shows a dominant linear dependence of  $I_{\text{FB}}$  on  $U_{\text{HV}}$  (the  $U_i$  were chosen to be approximately equidistant) due to the motional field effect, while the asym-

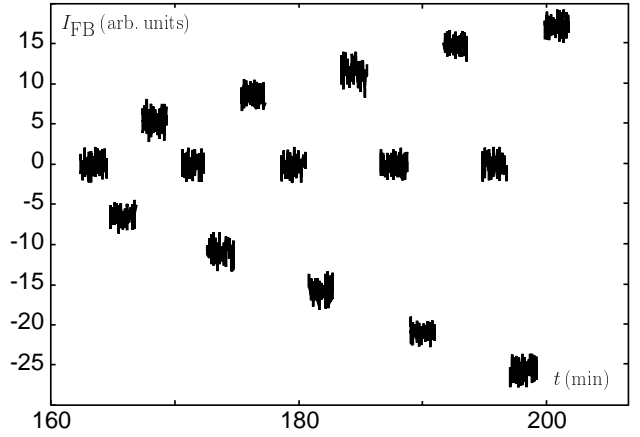


FIG. 2: Extract from an experimental run. The data acquisition software applies five different (approximately equidistant) voltages  $\pm U_i$ ,  $i = 1, \dots, 5$ , with both polarities. For each value of  $U_{\text{HV}}$ ,  $I_{\text{FB}}$  is recorded over 2 minutes. The figure shows a sequence  $U_{\text{HV}} = 0, +U_1, -U_1, 0, +U_2, -U_2, \dots$

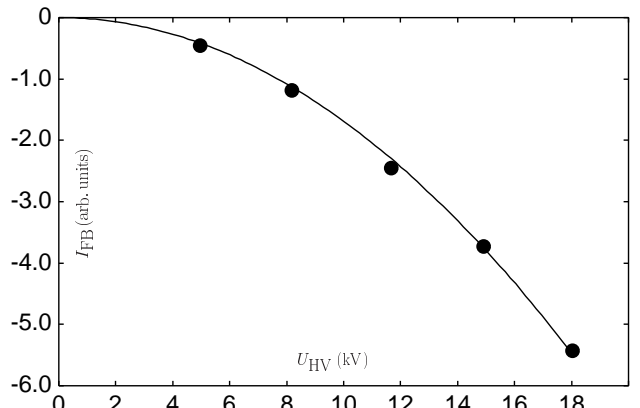


FIG. 3: Quadratic Stark shift due to tensor polarizability after offset and motional field subtraction. The (vertical) statistical error bar of each data point corresponds to the dot size.

metry of data recorded with positive and negative high voltage is due to the tensor polarizability. In the off-line data analysis the average value of  $I_{\text{FB}}$  for each high voltage is computed. Then the difference of time consecutive measurements with and without high voltage are calculated in order to subtract base line drifts and finally the values thus obtained for consecutive measurements with reversed polarities are averaged in order to eliminate the contribution from the motional field effect. The resulting averaged values then show a pure quadratic dependence on  $U_{\text{HV}}$  as illustrated in figure 3.

A simple quadratic fit to the data points allows, together with the calibration constants  $\beta$  and  $\varepsilon$ , to infer  $\alpha_2$  using equation 5 with a typical statistical error of 1% per run. The magnetic calibration constant  $\beta$  was inferred from the Ramsey fringe pattern with a precision

of 0.3%, while the electric calibration constant  $\varepsilon$  was determined by a semi-empirical method involving both numerical calculations using an adaptive boundary element method and the Aharonov–Casher phase shift (precision of 0.3%). Details of these calibration procedures will be published elsewhere [12].

The automated measurements have allowed us to study different systematic effects. No significant dependence of the results on doubling or halving the pump laser intensity was found. This proves that the beam is fully polarized in the  $|F = 4, M_F = 4\rangle$  hyperfine state, which is a prerequisite for the validity of equation 3. There was also no detectable dependence of the results on slight misalignments of the quarter-wave plates producing the circularly polarized light, nor on variations of the oven temperature and hence the velocity distribution of the beam. Variations of the probe intensity yielded no effect on the obtained results. There is however a serious systematic uncertainty, which currently limits the absolute precision of the results. Equations 4 and 5 were derived by assuming that the magnetic and electric fields are perfectly parallel. The orientation of the electric field was realized by a mechanical rotation of the electrode structure and could be determined with an accuracy of better than 1%. For historical reasons the rotated magnetic field was realized by adding the fields of two orthogonal pairs of coils. The contribution from the uncertainty ( $2.5^\circ$ ) of this alignment to the final result was estimated from a systematic experimental study. The uncertainties for  $\varepsilon$ ,  $\beta$  and  $\vartheta$ , together with the dominating error from the relative orientation of the  $\mathcal{E}$  and  $B$  fields yield a (conservative) upper bound for the total systematic uncertainty of 7.5%.

After averaging five runs the overall statistical error is 0.7%, which leads to the preliminary result of

$$\alpha_2(F = 4)/h = -3.34(2)(25) \cdot 10^{-8} \frac{\text{Hz}}{(\text{V}/\text{cm})^2},$$

where the numbers in parentheses give the statistical and systematic errors respectively. The value of  $\alpha_2(F = 4)$  inferred from previously reported [3] experimental results is

$$\alpha_2(F = 4)/h = -3.66(21)(7.3) \cdot 10^{-8} \frac{\text{Hz}}{(\text{V}/\text{cm})^2}$$

while the theoretical prediction from [4, 5] quoted in the article by Gould et al. [13] is

$$\alpha_2(F = 4)/h = -4.133 \cdot 10^{-8} \frac{\text{Hz}}{(\text{V}/\text{cm})^2}.$$

## CONCLUSION AND OUTLOOK

We have demonstrated a novel technique for the measurement of tensor polarizabilities in alkali atoms. We

have shown that with  $^{133}\text{Cs}$  a statistical precision below the 1% level can be achieved. The technique can easily be extended to other atoms by using suitable atomic beams and light fields. Our result is consistent with an earlier experimental result, and confirms the previously reported discrepancy with theoretical calculations at our current level of precision. In order to overcome the main current source of systematic error (parallelism of  $\vec{\mathcal{E}}$  and  $\vec{B}$ ), a new precision electrode arrangement with integrated magnetic field coils is currently under construction. With this improved set-up, a measurement of  $\alpha_2$  at the 1% level will be within reach.

The authors thank the mechanical workshop at the Physics Department of the University of Fribourg for their skillful support. We are indebted to J.-L. Schenker for his competent help with all kinds of electronic problems. We acknowledge the contributions of B. Schuh, M. Niering, and F. Rex in the early stage of this project. This work was financed in parts by grants of the Schweizerischer Nationalfonds (SNF) and the Deutsche Forschungsgemeinschaft (DFG).

---

\* Present address: Institut für Laser-Physik, Jungiusstrasse 9, D-20355 Hamburg, Germany

† Present address: Institut für Angewandte Physik, Wegelerstrasse 8, D-53115 Bonn, Germany

‡ Electronic address: antoine.weis@unifr.ch; URL: <http://www.unifr.ch/physics/frap/>

- [1] R. D. J. Haun and J. R. Zacharias, Phys. Rev. **107**, 107 (1957).
- [2] E. Simon, P. Laurent, and A. Clairon, Phys. Rev. **A57**, 436 (1998).
- [3] H. Gould, E. Lipworth, and M. C. Weisskopf, Phys. Rev. **188**, 24 (1969).
- [4] P. G. H. Sandars, Proc. Phys. Soc. **92**, 857 (1967).
- [5] J. R. P. Angel and P. G. H. Sandars, Proc. Roy. Soc. **A305**, 125 (1968).
- [6] A. Weis, J. Wurster, and S. I. Kanorsky, J. Opt. Soc. Am. **B10**, 716 (1993).
- [7] S. I. Kanorsky, A. Weis, J. Wurster, and T. W. Hnsch, Phys. Rev. **B10**, 1220 (1993).
- [8] A. Weis, B. Schuh, S. Kanorsky, and T. W. Hnsch, in *Technical Digest of European Quantum Electronics Conference 93*, edited by P. De Natale, R. Meucci, and S. Pelli (European Physical Society, Florence, 1993), p. 854.
- [9] B. Schuh, A. Weis, S. Kanorsky, and T. W. Hnsch, Opt. Commun. **100** (1993).
- [10] A. Grlitz, B. Schuh, and A. Weis, Phys. Rev. **A51**, 4305 (1995).
- [11] R. D. S. Swenumson and U. Ewen, Rev. Sci. Instrum. **52** (1981).
- [12] C. Ospelkaus, U. Rasbach, and A. Weis, to be published.
- [13] according to Equations 1 and 2 the shift rate  $\Delta\nu/\mathcal{E}^2$  reported in [3] has to be multiplied by 8/3 in order to infer  $\alpha_2(F = 4)$ .